

DTOKS: Tungsten and Beryllium Dust in ITER

M. Bacharis¹, M. Coppins¹, W. Fundamenski^{1,2}, J. E. Allen³

¹ *Imperial College, London, UK*

² *EURATOM/UKAEA Fusion Association, Culham Science Centre, Abingdon, UK*

³ *University College, Oxford, UK*

Introduction

Production of dust particles during tokamak operation is a critical issue for magnetic confinement fusion. Their introduction into the reactor can have serious consequence on its performance and can constitute a safety issue [1]. For these reasons the study of dust particles in tokamaks is crucial. Direct experimental observations of such particles that would give insight into their behaviour are quite challenging. In this context, numerical modelling of the relevant phenomena, such as in [2, 3], play a key role for better understanding the transport mechanisms of dust in tokamaks.

The plasma facing components in ITER will be Tungsten (W) and Beryllium (Be). In this work the dust transport code, Dust in TOKamakS (DTOKS) [2], will be used to investigate how far Tungsten and Beryllium dust grains can penetrate into the ITER plasma. First, a brief overview of the DTOKS model will be presented. Second, simulation results for ITER are examined. Dust grains of two different sizes, 10 and 100 microns, are injected from three different locations of the ITER vessel.

The DTOKS Code

DTOKS is a dust transport code developed at Imperial College [2]. It solves the equation of motion of a dust grain in a constant plasma background of the Scrape Off Layer (SOL). The code examines spherical dust grains. The physical model in DTOKS includes three parts: the dust grain charging model, the forces on the dust particle and a heating model including phase changes.

The charging model is based on the OML approach, modified for the case where the dust grain emits electrons [2, 4]. The forces considered include gravity, the Lorentz force and ion drag. The ion drag used in DTOKS is based on the Binary Collision (BC) approach [5] where both the ions scattered in the potential of the grain and the ones collected by the grain are taken into account. The heating model assumes the material properties of the dust grain are the same with the ones of the bulk material, additionally assuming that these remain constant and are not a function of temperature. The kinetic energy flux of the particles hitting the dust grain is then

	Mass ablated in Plasma in %		Mass ablated in Core in %	
	$10\mu m$	$100\mu m$	$10\mu m$	$100\mu m$
W outer divertor	28.64%	10.92%	$\ll 1\%$	$\sim 5\%$
Be inner divertor	99.56%	36.7%	$\ll 1\%$	$\ll 1\%$
W inner divertor	46%	23%	$\ll 1\%$	$\sim 2\%$
Be top	68.98%	65.97%	$\ll 1\%$	$\sim 1\%$

Table 1: A table of the mass ablated in the plasma and inside the last closed magnetic surface, in the core, normalized to the total mass injected for dust grains with a radius of $10\mu m$ and $100\mu m$ and an initial injection velocity of $v_{init} = 10m/s$ in the poloidal plane. An increase of the initial velocity would lead to dust penetrating further into the plasma.

calculated together with the fluxes due to ion backscattering, secondary electron and thermionic emission, neutral recombination and thermal radiation. Based on the calculated energy fluxes the temperature of the dust grain is computed. The model describing phase changes, is based on the temperature of evaporation/sublimation/melting, where the amount of material evaporating/sublimating/melting is calculated by balancing the energy fluxes on the dust grain with the energy needed for a sufficient amount of dust material to change phase.

W and Be Dust in ITER

This study involved the injection of dust grains with radius $10\mu m$ and $100\mu m$ from three different locations of the ITER vessel. These locations are the outer and the inner divertor and the top of the vessel. The electron Debye length is of the order of the $10\mu m$ particles, and it is smaller compared with the $100\mu m$ ones. The choice of dust materials injected from each location was chosen to be representative of that location. As already mentioned, the divertor in ITER will be W whereas the main vessel will be Be. For this reason W is injected from the outer divertor and Be from the top of the vessel. In the case of the inner divertor both W and Be dust particles are injected because of the amount of Be projected to be deposited in the inner divertor due to transport from other parts of the tokamak.

The injection velocity of the particles was $v_{init} = 10m/s$ in the poloidal plane, see [3]. The choice of the exact injection point, in the case of the inner and outer divertors, was chosen to be the estimated point of maximum energy flux to the divertor wall, as it was considered that the probability of dust production would be larger where thermal stresses on the wall's surface are large. In the case of the top of the vessel the highest point of the plasma background was chosen as an injection point. The particles in these series of simulation runs have been injected in the

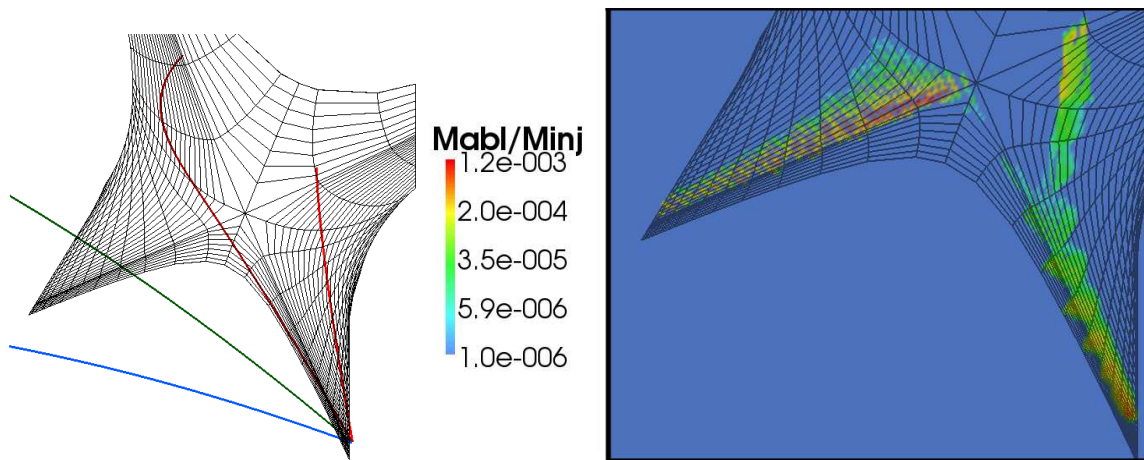


Figure 1: Representative dust trajectories (right) and a plot of the mass of dust ablated in the plasma (M_{abl}) as a fraction of the total injected mass (M_{inj}) by a cosine distribution of Tungsten particles with a radius of $100\mu m$ injected from the outer divertor (left).

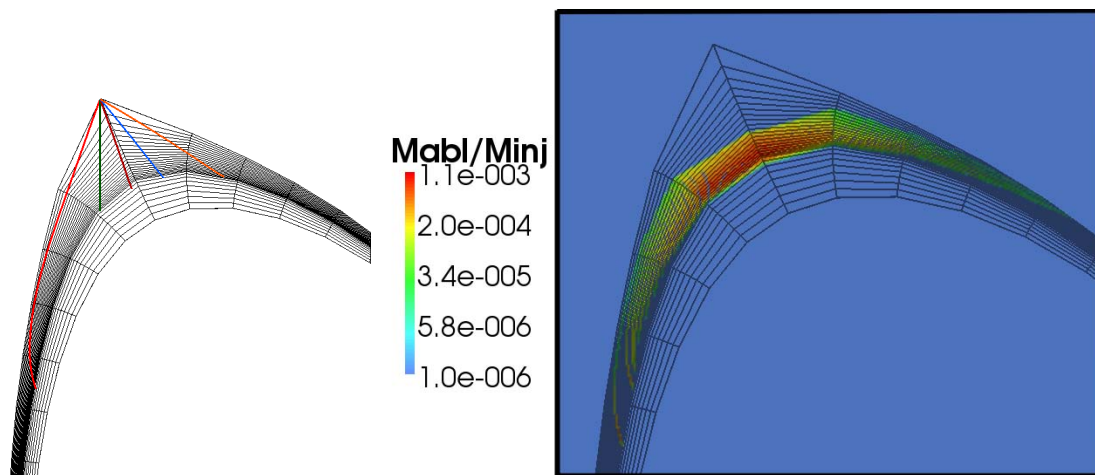


Figure 2: Representative trajectories (right) and a plot of the mass of dust ablated in the plasma (M_{abl}) as a fraction of the total injected mass (M_{inj}) by a cosine distribution of Beryllium particles with a radius of $100\mu m$ injected from the top of the vessel (left).

poloidal plane from -90 to +90 degrees, with respect to the normal, in one degree steps. The results are presented in Table 1 in the form of the percentage of the mass of the injected dust particles ablated in the plasma and also the fraction deposited within the separatrix, in the core. Also, two examples of the simulation results, one for W and one for Be, are presented in Figures 1 and 2. In these two Figures, the results are presented using both representative trajectories and with the help of a colour surface plot giving the amount of dust material ablated in a specific spot normalised to the total injected mass. This plot is the mass that has ablated in a specific computational cell and it depicts the probability of ablation of a dust particle in a specific place if that initial particle were injected from the same injection point with the same initial speed. However, in order to produce these surface plots, a distribution for the initially injected particles must also be included, in our case a cosine probability distribution typical for rough surfaces was chosen [2].

Conclusions

By examining the results depicted in in Table 1 and in Figures 1 and 2 for dust injected with an initial velocity of $v_{init} = 10m/s$, it can be seen that within the current bounds of the DTOKS model both W and Be dust grain can reach the area within the separatrix, the size of dust for which this is possible is $100\mu m$ for both W and Be (only in the case of top injection) dust grains. Furthermore, it is indicated that the majority of material injected as dust from the divertor regions is redeposited on the walls and only a small fraction ablates in the plasma. The proportion of redeposited material is a function of grain radius and increases for larger dust grains. In the case of dust injection from the top of the vessel the majority of the material is ablated in the plasma, with this proportion staying approximately constant even for larger dust grains. This difference can be attributed to the difference in the plasma geometry in the two regions, more uniform in the case of the top injection, and also the proximity to the injection point of high density and temperature regions. It must be also pointed out that an increase of the initial injection velocity would lead to dust penetrating further into the plasma.

This work was funded by the UK Engineering and Physical Sciences Research Council.

References

- [1] D. A. Mendis. *Plasma Sources Science Technology*, 11(26), 2002.
- [2] J. D. Martin, M. Bacharis, M. Coppins, G. F. Counsell, and J. E. Allen. *EPL*, 83(6), 2008.
- [3] A. Y. Pigarov, S. I. Krasheninnikov, T. K. Soboleva, and T. D. Rognlien. *Physics of Plasmas*, 12(12), 2005.
- [4] G. L. Delzanno, A. Bruno, G. Sorasio, and G. Lapenta. *Physics of Plasmas*, 12(6), 2005.
- [5] V.E. Fortov, A.V. Ivlev, S.A. Khrapak, A.G. Khrapak, and G.E. Morfill. *Physics Reports*, 421(1-2), 2005.